Simultaneous electrochemical-electron spin resonance measurements. I. Cell design and preliminary results

Ira B. Goldberg, and Allen J. Bard

J. Phys. Chem., **1971**, 75 (21), 3281-3290• DOI: 10.1021/j100690a013 • Publication Date (Web): 01 May 2002

Simultaneous Electrochemical-Electron Spin Resonance Measurements.

I. Cell Design and Preliminary Results

by Ira B. Goldberg and Allen J. Bard*

Department of Chemistry, The University of Texas at Austin, Austin, Texas 78712 *(Received May 5, 1971)*

Publication costs assisted by the Robert A. Welch Foundation

A cell was designed which allows precise control of electrochemical variables during *intra muros* electrogeneration of radical species in the cavity of an esr spectrometer. The advantages of simultaneous electrochemical-esr (SEESR) experiments are discussed, and results of potential step, current step, and cyclic voltammetric experiments on dimethylformamide solutions of anthraquinone, azobenzene, and nitrobenzene are described. Applications to the detection of short-lived electrogenerated radicals using signal-averaging techniques, to the measurement of the kinetics of reactions of electrogenerated radicals, and to the observation of secondary radicals are also discussed.

Introduction

Electrochemical generation of radicals and their detection by electron spin resonance (esr) spectroscopy has been used routinely for the last 10 years. Adams[1] and Kastening[2] have reviewed the most recent developments in this area, and several books[3] provide descriptions of the conventional apparatus required for these experiments. Recently other spectroscopic measurements have been combined with electrochemical experiments such as optical spectroscopy using optically transparent electrodes.[4] Combining electrochemistry with spectroscopy allows more confident identification of intermediates and products and enables the elucidation of mechanisms and the evaluation of kinetic parameters. When spectroscopic-electrochemical methods are combined, careful control of the electrochemical parameters is necessary to ensure that only the desired process is occurring in the zone of detection of the spectrometer. This is difficult to achieve when esr spectroscopy and electrochemistry are combined because of the high resistance of the thin cell[5,6] which must be used when radicals are generated in the microwave cavity. As a result, electrochemical generation in esr spectroscopy has been used primarily as a purely qualitative technique. Most precise esr measurements of the electrochemical behavior of systems has been carried out by generating the radicals away from the microwave cavity and then allowing some of the solution to flow into the cavity at a known rate.[7-9] Here the problems of cell resistance are avoided since an efficient electrochemical cell may be used.

Several kinetic measurements have been carried out by generating the radical inside of the microwave cavity. The behavior of the nitrobenzene anion radicals in aqueous solution was studied by Koopman and Gerischer.[10] In this case because the specific resistance of the solution was sufficiently low, the electrochemical behavior could be controlled. Hirasawa, *et al.*,[11] were able to obtain spectra and kinetic curves of radicals in nonaqueous systems by using a constant current passed through a solution which was flowing rapidly through the cell in the microwave cavity. To minimize electrical resistance, two parallel electrodes were placed in the cell. By using a computer of average transients either esr spectra or signal intensity–time curves could be recorded. Because of the flowing solution, the current distribution along the electrode was not uniform so that kinetic parameters could not be determined. Moreover, no controlled potential experiments were reported.

There have been few discussions of the dynamics of radical generation in conventional electrochemical-esr cells. Usually electrolysis inside of the microwave

(1) R. N. Adams, *J. Electroanal. Chem.*, **8**, 151 (1964).

(2) B. Kastening, *Chem. Ing. Tech.*, **42**, 190 (1970).

(3) C. P. Poole, "Electron Spin Resonance," Interscience, New York, N. Y., 1967, pp 624–633; R. S. Alger, "Electron Paramagnetic Resonance," Interscience, New York, N. Y., 1968, pp 267–272.

(4) See, *e.g.*, G. C. Grant and T. Kuwana, *J. Electroanal. Chem.*, **24**, 211 (1970), and references therein.

(5) D. H. Geske and A. H. Maki, *J. Amer. Chem. Soc.*, **82**, 2761 (1960).

(6) L. H. Piette, P. Ludwig, and R. N. Adams, *Anal. Chem.*, **34**, 916 (1962).

(7) B. Kastening, *Ber. Bunsenges. Phys. Chem.*, **72**, 20 (1968); B. Kastening and S. Vavricka, *ibid.*, **72**, 27 (1968); B. Kastening, *Collect. Czech. Chem. Commun.*, **30**, 4033 (1965); B. Kastening, *Z. Anal. Chem.*, **224**, 196 (1967).

(8) K. Umemoto, *Bull. Chem. Soc. Jap.*, **40**, 1058 (1966).

(9) D. Kolb, W. Wirths, and H. Gerischer, *Ber. Bunsenges. Phys. Chem.*, **73**, 148 (1969).

(10) R. Koopman and H. Gerischer, *ibid.*, **70**, 118 (1966); R. Koopman, *ibid.*, **70**, 121 (1966); R. Koopman and H. Gerischer, *ibid.*, **70**, 127 (1966).

(11) R. Hirasawa, T. Mukaibo, H. Hasegawa, N. Odan, and T. Maruyama, *J. Phys. Chem.*, **72**, 2511 (1968); R. Hirasawa, T. Mukaibo, H. Hasegawa, Y. Kanada, and T. Maruyama, *Rev. Sci. Instrum.*, **39**, 935 (1968).

cavity is carried out with a static solution where an essentially constant current is used. In the typical commercial electrochemical-esr cells[12] the cell resistance is about 1500 Ω/cm of cell length in 0.1 *M* aqueous potassium chloride, and 5000 Ω/cm in 0.1 *M* TBAI–DMF based on a value of about 250 Ω·cm for the specific resistance of 0.1 *M* TBAI–DMF. In ethereal solutions the cell resistance may exceed 100,000 Ω/cm. With a current of only 100 μA, the voltage drop along the electrode would be as high as 0.5 V/cm in DMF solutions. Thus, it is possible for more than one process to occur simultaneously at the electrode. Furthermore, it is not meaningful to attempt a controlled potential experiment, especially in this cell when the reference electrode is above the working electrode. The potentiostat would control only that portion of the working electrode closest to the reference electrode, and the potential would still vary along the rest of the length of the working electrode. Furthermore, there is a large uncompensated resistance (resistance between the working and reference electrode in the current path) so that a small change of current causes a large change in the regulated cell potential.

Dohrmann and Vetter[13] attempted to calculate the minimum lifetime of a radical which could be detected when generated in a conventional electrochemical-esr cell. They suggested that a rapid flow of solution through the cell and a small electrode placed at the center of the cavity would give the greatest signal for a rapidly decaying radical, if the potential of the electrode could be maintained on the plateau of the electrochemical wave of the radical formation. They estimated that if a current density of 0.1 A/cm^2 could be maintained by rapid flow of solution, then a radical with a lifetime of about 10^{-5} sec could be observed.

The purpose of this paper is (1) to present a cell in which the esr signal may be recorded while any of a variety of electrochemical experiments are carried out, *i.e.*, the cell potential may be controlled accurately so that the esr signal or a spectrum which corresponds to that potential, is obtained; (2) to study the behavior of stable radicals formed electrochemically by constant current, at constant potential, and during cyclic linear sweep voltammetry to find the upper and lower limits of time during which radicals can be studied; and (3) to explain briefly the dynamics of conventional internal generation and to contrast this method with the method presented here.

Experimental Section

Chemicals. Dimethylformamide (DMF), obtained from Baker Chemical Co., was purified by distillation at 15 mm from cupric sulfate onto molecular sieves three times. The solvent was then stored under helium atmosphere. The purity was checked periodically by voltammetry on a blank sample. The 9,10-anthraquinone (99.5% pure), obtained from Matheson Coleman and Bell, was used without purification. Azobenzene, obtained from Eastman, was recrystallized twice from 95% ethanol. The purified nitrobenzene, obtained from Baker, was dried by passing directly through an alumina column. Tetrabutylammonium iodide (TBAI) and tetrabutylammonium perchlorate (TBAP) were obtained from Southwestern Analytical Chemicals polarographic grade and were used as received, except that TBAP was dried under vacuum at 145° for 24 hr and stored over Drierite.

Instrumentation. Electron spin resonance measurements were conducted with a Varian V-4502 spectrometer equipped with a 9-in. magnet, 100-kHz field modulation, dual cavity, and a low noise-high power klystron. Electrochemical measurements were carried out in either of two ways. Cyclic chronopotentiometry, cyclic voltammetry, and controlled potential generation were done with a Princeton Applied Research Model 170 electrochemical instrument. Constant current pulses were applied either with the above instrument or by using a Tektronix Pulse Generator, Model 162, and a dropping resistor. In this case, the cell potential was monitored by connecting the reference electrode to a follower constructed with a Philbrick P65 operational amplifier. Simultaneous esr and electrochemical data were recorded with a dual-channel chart recorder. When necessary, a Nuclear Data Enhancetron 1024 was used for signal averaging. A block diagram of the apparatus set up for signal averaging is shown in Figure 1.

Cell Design. The design of the cell for simultaneous esr and electrochemical measurements is extremely critical. For a rectangular microwave cavity, it is necessary that the cell be fairly thin (about 0.05 cm for aqueous solution, 0.1 cm for materials with dielectric constants in the order of 40, and 0.2 cm for solvents with dielectric constants between 6 and 12). Since a low electrolyte resistance even in most aqueous systems is, therefore, nearly impossible, it is important to optimize the electrochemical behavior of the cell, bearing in mind the considerations of maximum esr response.

A diagram of the complete cell assembly is shown in Figure 2. Since DMF, with a dielectric constant of about 37, was used in these experiments, a cell thickness of 0.1 cm was chosen. The walls were constructed of 0.1-cm optical Pyrex. Two tungsten rods (0.075 cm diameter) were placed along the edges of the cell, with a U-shaped rod at the bottom of the cell to hold the long rods parallel. These rods served as the counterelectrode and must be kept as parallel as possible to ensure a uniform current density through the solution. The working electrode was made from a piece of platinum

(12) For example, Varian V-4556 or E-246 (cell dimensions 4 × 0.9 × 0.05 cm), Brucker BER-400 2E, or Jeolco JES-EL10.

(13) J. K. Dohrmann and K. J. Vetter, *J. Electroanal. Chem.*, **20**, 23 (1969).

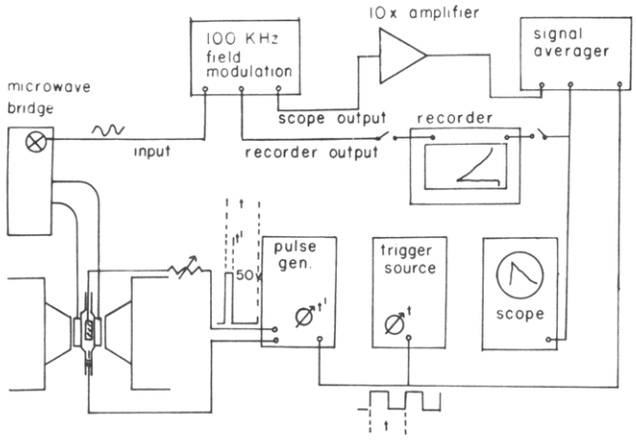

Figure 1. Block diagram of the esr apparatus used in pulse electrolysis experiments with signal averaging.

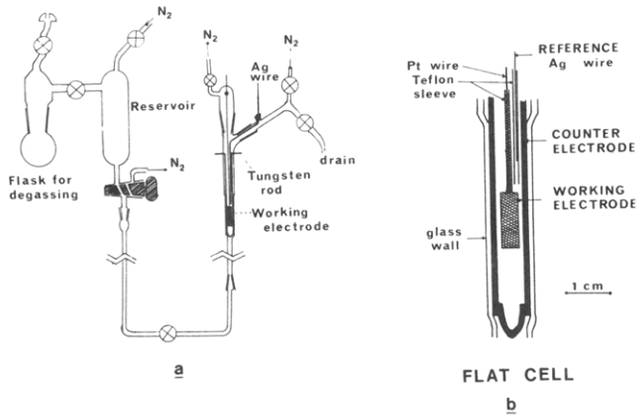

Figure 2. (a) Electrochemical cell and reservoir assembly. (b) Detail of flat cell portion of cell.

mesh, with a grid of 1 mm. Various widths between 0.2 and 0.4 cm, and lengths between 0.5 and 1.5 cm were used. A length of 0.025-cm diameter platinum wire was spot-welded to the mesh, and the wire was passed through a length of 0.038-cm i.d. Teflon tubing which was filled with epoxy. This prevented the long lead to the working electrode from being exposed to the solution. Contact to the electrochemical source was made above the solution level—the stopcock near this connection (Figure 2a) allows the whole cell to be flushed with nitrogen, but when closed, positive pressure keeps the solution level below the connection.

For the reference electrode, a length of 0.012-cm diameter silver wire was passed through a length of 0.038-cm i.d. Teflon tubing until the edge of the silver was 3–5 mm above the end of the Teflon. The Teflon sheath which filled with solution was fixed in place as shown.

Great pains were taken in the assembly of the cell to prevent slow leaks or solution movement within the cell. If one considers a small amount of radical at the region of maximum sensitivity, then to decrease the signal to one-half of the maximum value, the radical need only move about 5 mm in either direction. This would correspond to a loss of only 30 μl of solution. Thus, if a signal which decays by less than 5% within 30 sec is desired, a maximum rate of flow out of the cell would be about 1.0 μl/sec (4 ml/hr).

One consideration to be made in using this cell is the size of the working electrode. If it is desired to study fast kinetics, a long electrode which fills the cavity is desirable to obtain the maximum amount of radical. On the other hand, this should be kept as narrow as possible, since there will be solution resistance between the edge and the center of the electrode. If it is desired to follow chronopotentiometric or cyclic voltammetric experiments, a shorter and wider electrode will be useful since the current passed will be smaller and less uncompensated cell resistance will result. For any specific application, there must be a compromise between maximum electrode area and minimizing the resistive drop. The sensitivity along the length of the cavity parallel to the electrode follows an expression of the form $\cos^2(2\pi x/l)$, where l is the length of the cavity (2.3 cm) and x is the distance measured from the center of the cavity. If the electrode is centered in the cavity, then an electrode 11 mm long will allow a signal of 82% of the theoretical maximum while an electrode 6 mm long will give 50% of the theoretical maximum signal.

Procedure. Each solution was prepared under a nitrogen atmosphere. The solution was degassed by the freeze–pump–thaw method in the round-bottom flask attached to the reservoir (Figure 2). Helium was then allowed to enter above the solution. After the cell was assembled in the esr spectrometer, the reservoir was flushed with dry nitrogen, and the solution was transferred to the reservoir. The reservoir was then connected to the cell. Dry nitrogen was used to flush the apparatus, and the solution was allowed to flow into the cell. The experiments were done under a nitrogen atmosphere. For each electrochemical experiment, fresh solution was allowed to enter the cell.

Results and Discussion

A first test of any system which is designed for dual spectroscopic-electrochemical studies involves the investigation of stable systems in order to determine the range of usefulness of the system. If such an apparatus is to be used for kinetic studies, then stable radicals must not be removed from the zone of detection of the spectrometer by either convection or leakage or by chemical reaction with materials inherent in the cell design (*e.g.*, oxygen, products from the auxiliary electrode, etc.). To examine this cell, three substances which produce stable radicals in DMF were selected. The first 9,10-anthraquinone (AQ) exhibits two reversible electron transfer steps in aprotic media.[14]

(14) P. H. Given, M. E. Peover, and J. M. Schoen, *J. Chem. Soc.*, 2764 (1958).

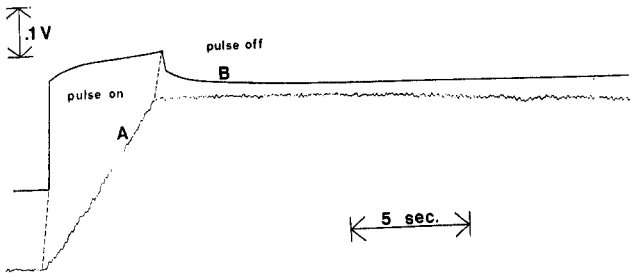

Figure 3. Esr signal (A) and electrode potential (B) during and following a constant current pulse of 200 μA. The solution contained 10.9×10^{-3} M anthraquinone and 0.105 M TBAI in DMF.

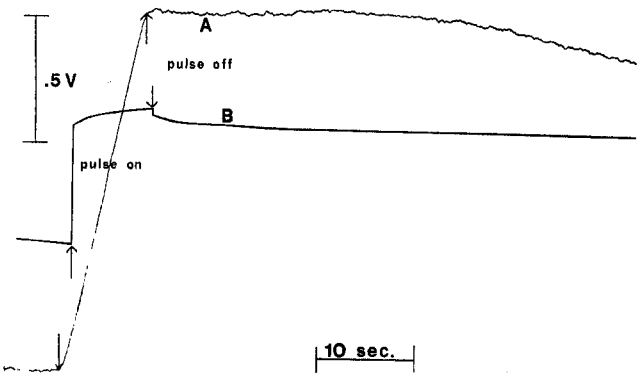

Figure 4. Esr signal (A) and electrode potential (B) during and following a constant current pulse of 200 μA. The solution contained 7.63×10^{-3} M nitrobenzene and 0.106 M TBAI in DMF.

Both the anion radical and the dianion are stable in DMF for at least several minutes. Nitrobenzene (NB) shows a reversible one-electron wave.[15] The second wave which is irreversible begins near the cathodic limit of 0.1 M TBAI–DMF and merges with background. The third substance, azobenzene (AB), also exhibits two one-electron reduction waves in DMF.[16] The radical anion is stable only for several seconds, but the dianion is rapidly protonated by the solvent to form hydrazobenzene.

Current Steps (Chronopotentiometry). Figures 3 and 4 show low current pulses applied to solutions of AQ and NB. Both the esr signal and the cell potential are recorded simultaneously. In both cases a stable signal is observed for 20 to 30 sec after the generation was terminated. The cell potential also remains nearly constant after the current is switched off. When the current is stopped, a small, rapid decrease of the cell potential is observed which arises from the small uncompensated cell resistance between the working and reference electrodes. With a current of 200 μA, this voltage change is between 20 and 40 mV (depending upon the exact position of the reference electrode) which corresponds to an uncompensated resistance of 100 to 200 Ω in this system.

Transition times were measured for AQ at applied current of 100, 200, and 500 μA. The theory of chronopotentiometry predicts that $i\tau^{1/2}/C$ (where i is the current, C is the concentration, and τ is the transition time) is expected to be constant. A value of 0.075 ± 0.015 A $\text{sec}^{1/2}$ M^{-1} was obtained from measurements at several concentrations. The results of these experiments are given in Table I. The evaluation of the transition time constant allows the establishment of the maximum time which a constant current pulse may be applied without a second process occurring.

Table I: Chronopotentiometric Transition Times for Anthraquinone in 0.1 M TBAI–DMF Solutions[a]

Anthraquinone concn, mM	Current (i), μA	Trans. time (τ), sec	$i\tau^{1/2}/C$, A $\text{sec}^{1/2}$ M^{-1}
5.25	100	16.0	0.077
4.59	100	8.6	0.064
4.59	200	3.8	0.085
4.59	500	0.5	0.08
10.90	200	14.6	0.071

[a] Electrode area about 0.2 cm^2.

Short pulses may also be applied to this system. Figure 5 shows a high current (25 mA) for 6.3-msec pulse applied to AQ. Because of the short pulse duration, signal averaging was required to obtain sufficient resolution to show the rising portion of the curve.

Similar experiments with azobenzene did not give a steady esr signal after the generation of radicals (Figure 6); here the signal decayed after the termination of the current pulse with a half-life of about 23 sec. Sadler and Bard[16] found that 1.10 to 1.16 F/mol were required to reduce azobenzene completely to the anion radical by controlled potential coulometry. Upon coulometric oxidation, 70% of the material was recovered. The rapid initial decay found with esr measurements suggests that the anion radical reacts with some species in the solvent–electrolyte system, but larger amounts of the anion radical are stable.

Reversal chronopotentiometry was selected as one of the quantitative tests for studying the electrochemical behavior of the cell. When the product generated with a constant current at an electrode is stable, and semi-infinite linear diffusion conditions exist, the time required to reach a transition upon current reversal, t_r, is related to the forward generation time t_f ($t_f \leq \tau$) by $t_r = t_f/3$.[17] On the other hand, if the same experiment is carried out in a thin layer cell,[18] then $t_r = t_f$.

(15) T. Kitagawa, T. P. Layloff, and R. N. Adams, *Anal. Chem.*, **35**, 1086 (1963).

(16) (a) J. L. Sadler and A. J. Bard, *J. Amer. Chem. Soc.*, **90**, 1979 (1968); (b) G. G. Aylward, J. L. Garnett, and J. H. Sharp, *Anal. Chem.*, **39**, 457 (1967).

Table II: Results of Reversal Chronopotentiometry in 0.10 M TBAI–DMF Solutions

	i, μA	Time, forward, (t_f), sec	Time, reverse, (t_r), sec	t_r/t_f	Esr signal at t_f, S_f	Esr signal at t_r, S_r	S_r/S_f
7.68×10^{-3} M nitrobenzene	100	33.5	6.5	0.20	7.09	5.67	0.80
	200	10.0	2.2	0.22	5.20	4.20	0.80
	200	9.5	2.1	0.22	8.15	6.35	0.78
4.59×10^{-3} M anthraquinone	100	2.95	0.77	0.26	4.36	3.25	0.75
	100	1.42	0.38	0.27	3.22	2.28	0.71
	200	3.96	0.92	0.23	6.75	5.20	0.77

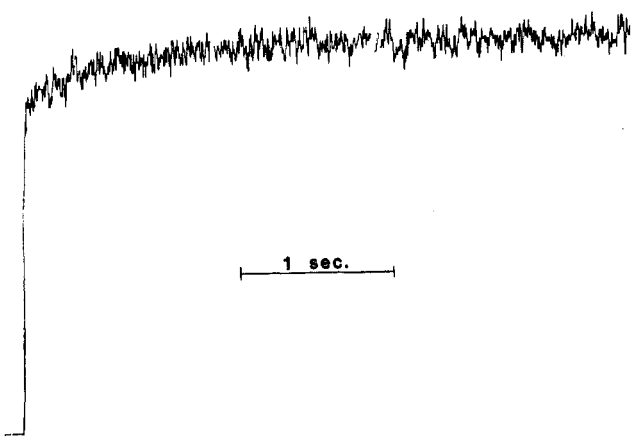

Figure 5. Esr signal (averaged four times) for a constant current pulse of 25 mA for 6.3 msec. The solution contained 4.66×10^{-3} M anthraquinone and 0.104 M TBAI in DMF.

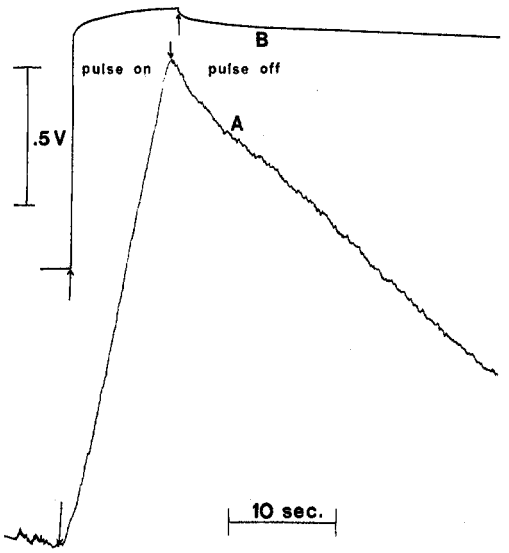

Figure 6. Esr signal (A) and cell potential (B) during and following a constant current pulse of 100 μA. The solution contained 5.50×10^{-3} M azobenzene and 0.102 M TBAI in DMF.

Figure 7 shows a typical current reversal study, and the results of several such experiments are summarized in Table II. In all cases the t_r/t_f ratio is less than 1:3. Normally, this is taken to indicate instability of the electrogenerated product, because decomposition of the product would decrease the amount available for the reverse electrode process. In this experiment, however, the esr signals at the time that the current is reversed (S_f at t_f), and at the reverse transition time (S_r at t_f) can also be compared. The data on Table II show that in all cases (within ± 0.01 units)

$$\frac{t_r}{t_f} = 1 - \frac{S_r}{S_f} \qquad (1)$$

Hence, the fraction of radical remaining in solution after the reversal is equal to the fraction of radical which is not reoxidized so that even though $t_r/t_f < 1/3$, no chemical reaction of the product occurs during the time of these measurements. Furthermore, there is no significant curvature of the lines which show the esr signal during the generation and oxidation of the anion radical. (Since both processes are carried out at constant current and 100% current efficiency, a linear rise and decay are expected.) The t_r/t_f ratio of less than one-third probably results from some convection occurring and removing product from the vicinity of the electrode. Double-layer charging may have an effect on these measurements at shorter times, but it is inadequate to explain the deviation from one-third at times greater than about 2 sec.

What occurs at the counterelectrode is an important consideration in using this cell. Figure 2 shows that both the counterelectrode and the working electrode are within the microwave cavity. If radicals were produced at the counterelectrode, then an esr signal from these would result. Radical formation at the counterelectrode was not observed in any of our experiments using TBAI as a supporting electrolyte. During reductions, iodine forms at the counterelectrode. During the oxidation step, iodine near that electrode inside the cavity as well as excess iodine re-

(17) (a) P. Delahay, "New Instrumental Methods in Electrochemistry," Wiley-Interscience, New York, N. Y., 1954; (b) T. Berzins and P. Delahay, *J. Amer. Chem. Soc.*, **75**, 4205 (1953).

(18) A. T. Hubbard and F. C. Anson in "Electroanalytical Chemistry," Vol. 4, A. J. Bard, Ed., Marcel Dekker, New York, N. Y., 1969.

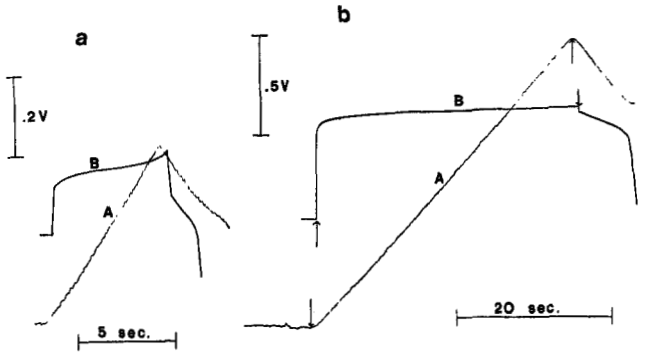

Figure 7. Esr signal (A) and cell potential (B) during reversal chronopotentiometry. (a) 200-μA pulse for 6 sec and reversal. The solution contained 10.9×10^{-3} M anthraquinone and 0.1 M TBAI in DMF. (b) 100-μA pulse for 32 sec and reversal. The solution contained 7.68×10^{-3} M nitrobenzene.

maining in solution above the flat cell portion but still in contact with the tungsten counterelectrodes is reduced before radicals are generated. Similar experiments in TBA–perchlorate–DMF solutions, however, where the counterelectrode oxidation products are not as stable as I_3^-, have shown that radicals can be produced at the tungsten nearest the working electrode. In cases when radical formation at the counterelectrode is possible, it may be necessary to add some nonradical producing electroactive substance (esr depolarizer) so that secondary radicals are not generated.

When currents are applied for long periods of time, one must consider the possibility of the products generated at the counterelectrode reacting with the radicals generated at the working electrode. The thickness of the diffusion layer is of the order of $3\sqrt{Dt}$, where D is the diffusion coefficient in square centimeters per second and t is the time of the generation. Since the counterelectrode is about 0.15 cm from the working electrode and assuming D to be 10^{-5} cm^2/sec, then the time required for materials generated at each electrode to diffuse through 0.075 cm when the substances would begin to react is about 60 sec. Convection can reduce this estimated time substantially, however.

When the current is passed for periods greater than the transition time τ, the potential will shift to allow secondary processes to occur. Figure 8 shows a long constant current pulse (with no current reversal) applied to a system containing AQ. For convenience, the figure may be divided into four sections. In section A, the only process which occurs is the reduction of AQ to its anion radical

$$AQ + e^- \longrightarrow AQ^{\cdot -} \qquad (2)$$

at 100% current efficiency and the esr signal shows a

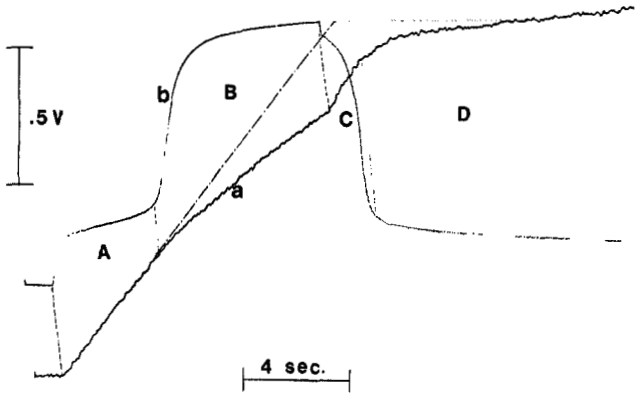

Figure 8. Esr signal (a) and cell potential (b) during and following a constant current pulse of 200 μA. The reduction to the anion and dianion are shown. The solution contained 4.59×10^{-2} M anthraquinone.

linear increase. During the interval section B the processes which occur at the electrode are

$$AQ^{\cdot -} + e^- \longrightarrow AQ^{2-} \qquad (3a)$$

which removes radicals from solution, and

$$AQ + 2e^- \longrightarrow AQ^{2-} \qquad (3b)$$

However, the formation of $AQ^{\cdot -}$ continues in the solution by the reaction

$$AQ^{2-} + AQ \longrightarrow 2AQ^{\cdot -} \qquad (4)$$

Here the esr signal increases at a decreasing rate since the rate of reaction 4 must be slower than the rate of reactions 3a and b. As reactions 3a and b proceed, (3a) becomes more significant with respect to (3b), since the flux of AQ toward the electrode decreases. When the current is stopped (section C), reaction 4 continues, since AQ is still diffusing toward AQ^{2-}, but AQ^{2-} is no longer being produced. Hence, the esr signal increases to a steady value. At the same time a rapid decrease of the cell potential is observed as AQ^{2-} is removed, and the potential becomes determined by the AQ,$AQ^{\cdot -}$ couple.

Section D shows both relatively steady esr signal and cell potential, since all of the AQ^{2-} has now diffused away from the electrode and reacted. The height of the line extrapolated from the initial buildup of radical (section A) to the time that the current is stopped corresponds to the flat portion of the esr signal in region D. This shows that the dianion AQ^{2-} is stable in this environment, and the net yield of $AQ^{\cdot -}$ in the steady-state esr signal is 100%.

Potential Steps. By applying a constant potential to the working electrode, the occurrence of secondary electrode processes are avoided. The results of these experiments show that the first 15–25 sec after a potential on the plateau of the electrochemical wave is applied to the cell, the current decays approximately as $t^{-1/2}$ and the esr signal increases at $t^{1/2}$ as predicted

by theoretical treatments.[17a] However, after this time the current approaches a steady value which is significantly greater than zero while the esr signal slowly increases. The magnitude of the steady-state current, which is probably the result of natural convection, is about 10–20 μA/mM with a 0.44-cm^2 electrode. In continuous constant current generation, as ordinarily employed in *intra muros* electrochemical esr techniques, this magnitude of current can be supported by convection, and secondary processes should not be significant. On several occasions after 2 or 3 min the current begins to oscillate slightly, again probably because of convection.

The potential step method has the advantage of maintaining the electrode at a constant potential, enabling exact control of the electrode process. Moreover, the maximum amount of radical per unit time will be generated by this technique. It is also possible to step to later waves and generate the dianion, dication, or secondary radicals at the electrode and examine their stability in solution.

Cyclic Voltammetry. Cyclic voltammetric studies with simultaneous recording of the esr signal can provide useful information about which electrolytic processes produce radicals and which involve their destruction. The previous current step and potential step experiments showed that the effects of convection become important after 15 to 25 sec, so that for quantitative current–voltage studies, each experiment must be limited to that time duration. If a scan of 1 V and a reversal is desired, the minimum scan rate would be about 20 mV/sec. Slower sweeps can be used for qualitative and semiquantitative studies. Consider qualitatively several representative cyclic voltammograms (Figure 9). The cyclic voltammogram of a system which exhibits a one-electron reduction (eq 5) is shown in Figure 9A. The variation of the esr signal

$$R + e^- \rightleftarrows R^{\cdot-} \qquad (5)$$

(S) with potential shows the following behavior: S increases when reduction begins and the maximum rate of increase of S is at the peak cathodic current (i_{pc}), noted by point a. The signal continues to increase and at point r, the potential sweep is reversed. The signal continues to increase until the current becomes anodic (*i.e.*, the radical is oxidized), denoted by point b. The maximum rate of decrease of the signal occurs near the peak anodic current (i_{pa}) (point c) with a continuous decrease of S as the potential is made more positive.

The current and esr signal as a function of potential for a system in which the radical ion decomposes

$$R^{\cdot-} \xrightarrow{\text{fast}} P \qquad (6)$$

is shown in Figure 9B. Here a buildup of radical is observed as in Figure 9A, but if the rate of decomposition is greater than the rate of electrolysis, the esr signal will

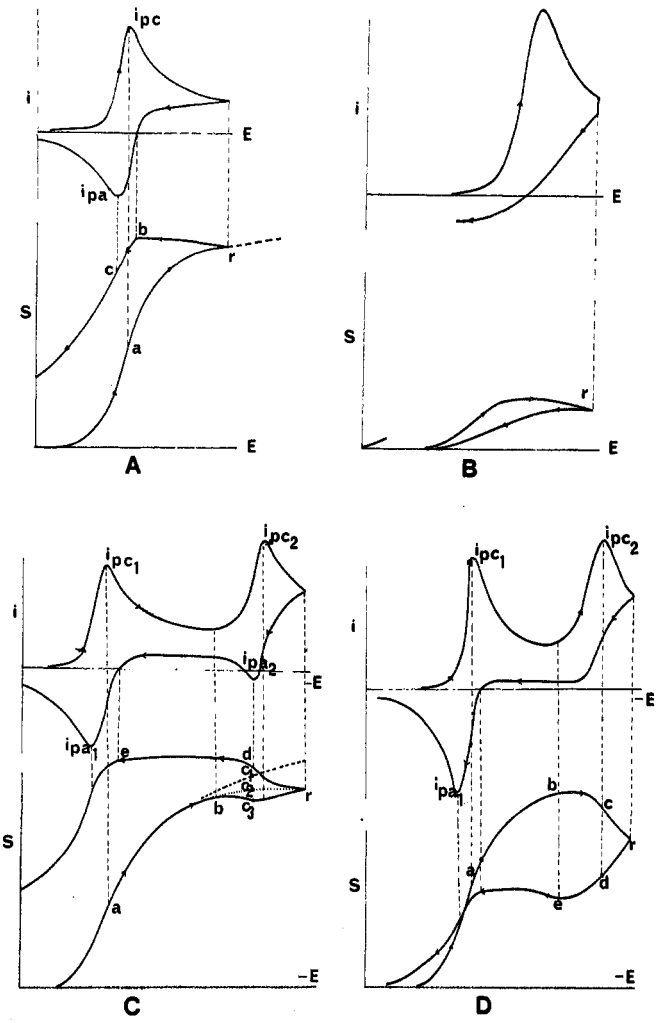

Figure 9. Current (i) and esr signal (S) for cyclic voltammograms representative of several typical electrochemical systems: (A) one-electron transfer and chemically stable and radical product; (B) one-electron transfer and unstable radical product; (C) two one-electron transfer steps with both radical and diamagnetic product stable; (D) two one-electron transfer steps with stable radical and unstable second product.

decrease following reversal. The fact that the radical is unstable is also indicated by the absence of an anodic current peak. Figures 9C and D show cyclic voltammograms for systems which exhibit two waves. The first wave corresponds to generation of a stable radical ion, and the second wave corresponds to the one-electron reduction of the radical anion to a stable dianion (eq 7).

$$R^{\cdot-} + e \rightleftarrows R^{2-} \qquad (7)$$

The current–voltage curve (Figure 9C), where the dianion is stable, shows two reduction waves and, on scan reversal, shows two oxidation waves. In this case S increases as in Figure 9A and will continue to increase until the reduction of the dianion begins (point b). After point b, the trend of S depends on the relative scan rate and diffusion coefficients. If the scan rate is fast, the diffusion layer is very thin, the flux of R coming toward the electrode is large, and S will continue

to increase (line b-c_2) because R^- is produced by reaction of R^{2-} with R (eq 8) more rapidly than it is removed by the reaction in eq 7. This increase

$$R + R^{2-} \longrightarrow 2R^- \quad (8)$$

would be less than the increase that would have been observed had the dianion not been generated (line b-c_1). On the other hand, if the scan rate is slow, so that the diffusion layer is broad, then the flux of R near the electrode is small and a decrease of S is observed (line b-c_3). A minimum would occur at approximately the same potential as the second reduction peak E_{pc2}. After this point the esr signal may again increase, because the rate of the reaction of R^- and R^{2-} becomes greater than that of the reduction of R^- at the electrode. After reversal at point r, when the cell potential again approaches E_{pa2}, S increases rapidly because of the oxidation of R^{2-} to R^- (point d). At point e, S decreases as the current becomes anodic.

A final case which can be considered is one in which the dianion is unstable in solution and decomposes to an electroinactive diamagnetic product Q (eq 9). The

$$R^{2-} \xrightarrow{\text{fast}} Q \cdot \quad (9)$$

current and esr signal are shown as a function of potential in Figure 9D. As before, S increases until point b where the second reduction begins. Now S increases until some potential between b and c where the rate of production of R^- at the electrode is smaller than the rates of reactions given by (7) and (9); at this point, S begins to decrease. The maximum rate of decrease of S will be near point c which corresponds to i_{pc2}. After reversal, S continues to decrease until the potential is again between points d and e. The point at which S begins to increase will depend upon the diffusion layer thickness, and therefore, the scan rate and the rate of decomposition of the dianion. As the potential again becomes more positive, S will follow the same trends as shown in Figures 9A and C.

Several experimental cyclic voltammetric studies with simultaneous recording of the esr signal are shown in Figures 10 and 12. Several typical scans on solutions of NB from 10 to 1 V/sec are shown in Figure 10. The results of cyclic voltammetry on fairly concentrated solutions of NB and AB are given in Table III. The $i_p/v^{1/2}$ values in Table III are not constant as predicted for a simple reversible electrode reaction.[19] There are probably several reasons for this inconsistency. At fast sweep rates, where the currents are high, the uncompensated cell resistance becomes important and the potential sweep departs from linearity.[20] Furthermore, at higher currents the ohmic voltage drop between the center and outside edges of the electrode becomes significant, and the effective electrode area becomes smaller. This resistance between the center and edge of the electrode is about 300 to 400 Ω with the widest electrode used (3.5 mm). On the other hand, at slow scan rates convection becomes a significant factor and higher peak currents result. In general, we find that lower concentrations give better constancy in the value of $i_p/v^{1/2}$ at faster sweep rates.

The variation of esr signal S with sweep rate v and peak current can be derived as follows. The current as a function of potential for a reversible charge transfer is given by eq 10[19]

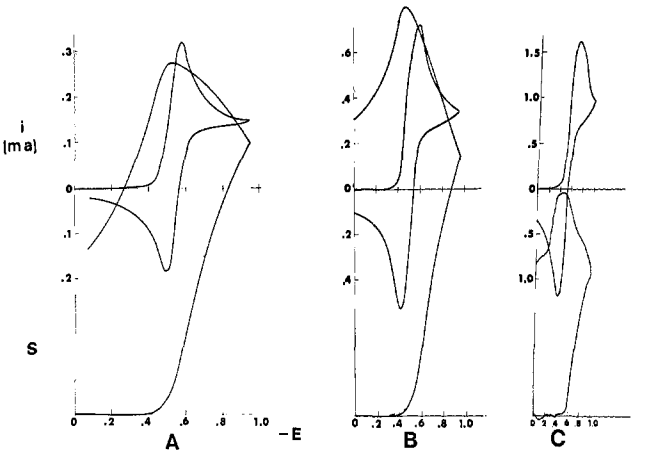

Figure 10. Experimental current (i) and esr signal (S) during cyclic voltammetry in a solution containing 7.68×10^{-3} M nitrobenzene: (A) 10 mV/sec; (B) 100 mV/sec; (C) 1 V/sec.

Table III: Cyclic Voltammetry–Esr Results

v, scan rate, mV/sec	i_{pc},[a] mA	i_{pa},[a] mA	i_{pc}/i_{pa}	S[a]	$i_p/v^{1/2}$
(a) 7.68 mM Nitrobenzene in 0.1 M TBAI-DMF					
5	0.237	0.230	0.97	13.80	3.34
10	0.315	0.308	0.98	11.90	3.15
20	0.410	0.385	0.95	9.54	2.90
50	0.565	0.555	0.98	5.34	2.52
100	0.717	0.717	1.00	3.58	2.26
200	0.910	0.910	1.00	2.23	2.03
500	1.25	1.25	1.00	1.37	1.77
1000	1.60	1.50	1.00	0.98	1.60
(b) 5.50 mM Azobenzene in 0.10 M TBAI-DMF					
5	0.164	0.145	0.88	8.65	2.32
10	0.209	0.185	0.89	5.89	2.09
20	0.270	0.238	0.89	3.10	1.91
50	0.385	0.360	0.93	2.97	1.76
100	0.480	0.460	0.96	1.89	1.54
200	0.642	0.632	0.98	1.26	1.44
500	0.882	0.880	0.99	0.72	1.25
1000	1.18	1.17	0.99	0.54	1.18

[a] i_{pc} is peak current in reduction, i_{pa} reversal peak current, and S = esr signal in arbitrary units.

(19) R. S. Nicholson and I. Shain, *Anal. Chem.*, **36**, 706 (1964).

(20) W. T. DeVries and E. VanDalen, *J. Electroanal. Chem.*, **10**, 183 (1965); R. S. Nicholson, *Anal. Chem.*, **37**, 667 (1965).

$$i = (nF)^{3/2}AC_0(\pi D_0)^{1/2}v^{1/2}\chi\left(\frac{nFvt}{RT}\right)\Big/(RT)^{1/2} \quad (10)$$

where t is the time from the beginning of the sweep, $\chi(nFvt/RT)$ is the "current function"[19] which is a function of the applied potential and the other symbols have their usual meanings. The number of coulombs passed during the potential sweep is

$$Q = \int i\mathrm{d}t = \frac{(nF)^{3/2}AC_0(\pi D_0)^{1/2}v^{1/2}}{(RT)^{1/2}}\int_0^t \chi\left(\frac{nFvt}{RT}\right)\mathrm{d}t \quad (11)$$

Substituting $E = vt$ and $\mathrm{d}t = E/v$ into (11) and using the expression for the peak current, i_p

$$i_p = \frac{(nF)^{3/2}AC_0(\pi D_0)^{1/2}v^{1/2}}{RT^{1/2}}\chi_{max} \quad (12)$$

where χ_{max} is the maximum value of the current function yields

$$Q = \left(\frac{i_p}{v}\right)\int_{E=E_1}^{E=E_2}\left[\chi\left(\frac{nFE}{RT}\right)\Big/\chi_{max}\right]\mathrm{d}E \quad (13)$$

Because the integral in eq 13 is only a function of the potential range of the sweep, then Q, and hence the esr signal, S, which is proportional to Q, should also be proportional to i_p/v. A plot of S, measured just before the scan reversal, *vs.* i_p/v is shown in Figure 11. A linear relationship exists from sweep rates of 1 V/sec until about 20 mV/sec. At sweep rates below 20 mV/sec, convection again interferes.

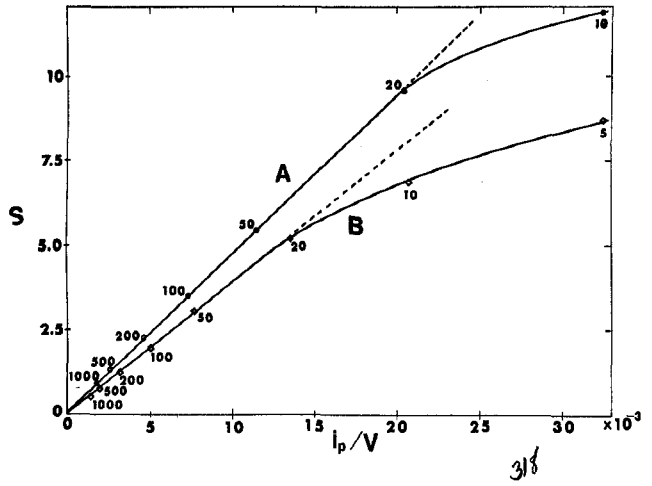

Figure 11. Esr signal (S) *vs.* the peak cathodic current divided by the sweep rate (i_p/v) for solutions of 7.68×10^{-3} M nitrobenzene (A) and 5.50×10^{-3} M azobenzene (B). Value of scan rate (millivolts per second) indicated on figure.

Experimental cyclic voltammograms involving two waves are shown in Figure 12. That of AQ (Figure 12) exhibits two reversible waves, and qualitatively resembles that of Figure 9C. By comparison, the cyclic voltammogram and esr signal of AB shown in Figure 12 is qualitatively similar to that of Figure 9D, except that

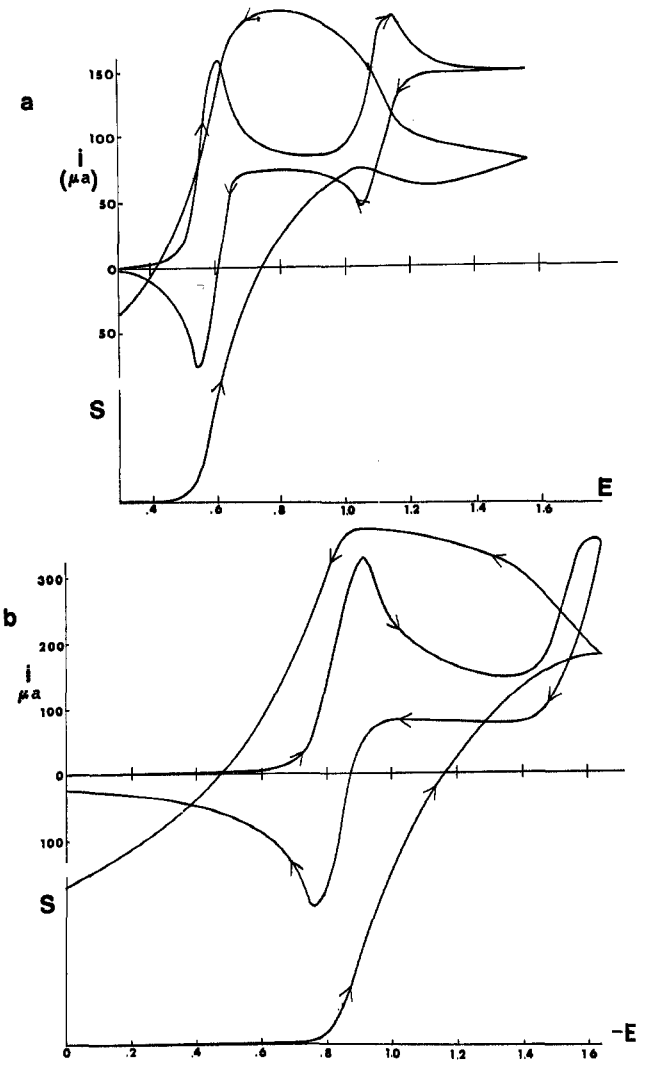

Figure 12. Esr signal (S) and current (i) during cyclic voltammetry: (a) solution of 6.43×10^{-3} M anthraquinone and 0.104 M TBAP in DMF, sweep rate 10 mV/sec; (b) solution of 5.50×10^{-3} M azobenzene and 0.103 M TBAI in DMF, sweep rate 20 mV/sec.

less AB^- was reduced to AB^{2-}, and that S did not decrease as much as in Figure 12.

Conclusions

The cell described is useful for simultaneous electrochemical-esr (SEESR) experiments for times up to about 20 sec. The application of these techniques to the study of the kinetics of decay of electrogenerated radicals requires a theoretical treatment of the expected signal–time behavior for various reaction schemes and reaction orders. A digital simulation[21] treatment of these is being carried out. The application of SEESR techniques to the detection of short-lived electrogenerated radicals, using signal averaging techniques, and to the elucidation of secondary reactions in electrolytic hydrodimerizations is currently under investigation.

(21) S. Feldberg, I. B. Goldberg, and A. J. Bard, unpublished research.

Acknowledgment. The support of the National Science Foundation (GP-6688X) and the Robert Welch Foundation is gratefully acknowledged. We also thank Mr. John Somerville for constructing the esr cell and Mr. Vincent Puglisi and Professor James R. Bolton for helpful advice and suggestions. The esr spectrometer was purchased under a grant from the National Science Foundation (GP-2090).

The Conductance and Association Behavior of Alkali Perchlorates in Water at 25° [1]

by Alessandro D'Aprano

Institute of Physical Chemistry, University of Palermo, Palermo, Italy *(Received June 29, 1970)*

Publication costs borne completely by The Journal of Physical Chemistry

The conductance of the alkali perchlorates at 25° has been measured in water in a concentration range up to 0.06 M and the experimental values analyzed by a revised Hsia–Fuoss (1967) conductance equation. Association increases with atomic number; it is negligible for lithium and marginal for sodium. For the other three alkali perchlorates, pair association constants are $K_A(K) = 1.0$, $K_A(Rb) = 1.35$, and $K_A(Cs) = 1.7$.

Introduction

Most previous work on the association of 1:1 electrolytes by conductometric methods was carried out in solvents or solvent mixtures in the range of dielectric constants below 30. In solvents of higher dielectric constant, and especially in water, association is slight and determination of the association constants is therefore difficult. The first estimate for 1:1 salts in water was made by Davies[2] who used the Onsager limiting coefficient plus an empirical term to estimate the conductance Λ_i of the free ions and then calculated the fraction γ of free ions as $\Lambda(obsd)/\Lambda_i$. Based on his "rather tentative values," he concluded that "salts containing a common anion fall, in strength, in the following order: Li > Na > K > Rb > Cs > Tl." More recently, a theoretical derivation[3,4] of the higher terms in the conductance function has been made, which permits a direct calculation of γ from conductance data. This method has been applied to data on the alkali halides in water[5,6] and to salts in mixtures of high dielectric constants.[7-9]

Previous conductometric measurements for alkali metal salts in dioxane–water,[10,11] in ethanol–water[12] mixtures, and in various hydrogen bonded solvents[13,14] have shown that in contrast with direct coulombic interactions, the association of these salts increases as the crystallographic radii of the cations increase. The association sequence found, namely Li < Na < K < Rb < Cs, has been explained by assuming that in hydrogen-bonded solvents, the alkali metal cations are extensively solvated. The same behavior has been postulated by Kay[15] for the association of alkali halides and perchlorates in aqueous solutions.

In order to test this assumption experimentally, the conductance of the alkali perchlorates has been measured in water in a concentration range up to 0.06 M, corresponding to the upper limit of applicability of the present theory. Three of the perchlorates (lithium, sodium, and potassium) have already been measured,[16] the curve for potassium perchlorates lies on the limiting

(1) Grateful acknowledgment is made to the "Consiglio Nazionale delle Richerche" for support of this research.

(2) C. W. Davies, *Trans. Faraday Soc.*, **23**, 351 (1927).

(3) R. M. Fuoss and L. Onsager, *J. Phys. Chem.*, **61**, 668 (1957).

(4) R. M. Fuoss and K. L. Hsia, *Proc. Nat. Acad. Sci. U. S.*, **57**, 1550 (1967); **58**, 1818 (1967).

(5) K. L. Hsia and R. M. Fuoss, *J. Amer. Chem. Soc.*, **90**, 3055 (1968).

(6) Y. C. Chiu and R. M. Fuoss, *J. Phys. Chem.*, **72**, 4123 (1968).

(7) A. D'Aprano and R. M. Fuoss, *ibid.*, **72**, 4710 (1968).

(8) A. D'Aprano and R. M. Fuoss, *J. Amer. Chem. Soc.*, **91**, 211 (1969).

(9) A. D'Aprano and R. M. Fuoss, *ibid.*, **91**, 279 (1969).

(10) T. L. Fabry and R. M. Fuoss, *J. Phys. Chem.*, **68**, 971 (1964).

(11) F. Accascina, A. D'Aprano, and R. Triolo, *ibid.*, **71**, 3469 (1967).

(12) R. L. Hawes and R. L. Kay, *ibid.*, **69**, 2420 (1965).

(13) R. L. Kay, *J. Amer. Chem. Soc.*, **82**, 2099 (1960).

(14) G. B. Porfitt and A. L. Smith, *Trans. Faraday Soc.*, **59**, 257 (1963).

(15) R. L. Kay in "Electrolytes," B. Pesce, Ed., Pergamon Press, New York, N. Y., 1962, p 119.

(16) J. H. Jones, *J. Amer. Chem. Soc.*, **67**, 855 (1945).